



HAL
open science

Distribution of Avalanches on the (n,k) -wheel

Dominique Rossin, Arnaud Dartois

► **To cite this version:**

Dominique Rossin, Arnaud Dartois. Distribution of Avalanches on the (n,k) -wheel. FPSAC/SFCA'03, 2003, Linkoping, Sweden. hal-00016372

HAL Id: hal-00016372

<https://hal.science/hal-00016372>

Submitted on 2 Jan 2006

HAL is a multi-disciplinary open access archive for the deposit and dissemination of scientific research documents, whether they are published or not. The documents may come from teaching and research institutions in France or abroad, or from public or private research centers.

L'archive ouverte pluridisciplinaire **HAL**, est destinée au dépôt et à la diffusion de documents scientifiques de niveau recherche, publiés ou non, émanant des établissements d'enseignement et de recherche français ou étrangers, des laboratoires publics ou privés.

Sandpile avalanche distribution on the wheel.

Arnaud Dartois^a and Dominique Rossin^b

^a*LIX, École polytechnique, 91128 PALAISEAU Cedex, FRANCE*

^b*CNRS, LIAFA, Université Paris 7, 2 Place Jussieu, 75251 PARIS Cedex 05, FRANCE*

Abstract

This paper deals with the sandpile model on the wheel, a lattice with particular boundary conditions. It presents how transducers applied to the language of recurrent configurations of the abelian sandpile model can help determining critical exponents of the underlying model. We present exact results for the avalanche distribution on the simple wheel, and give some clues for the multiple one where strange phenomena happen.

Key words: Sandpile model, avalanche, wheel, lattice, critical group

PACS: 45.70.Ht, 05.65.+b, 07.05.Tp, 61.43.Bn, 02.10.Ox

Introduction

The standard abelian sandpile model (ASM) was introduced by Bak, Tang and Wiesenfeld [1] in 1987. This model, based on a cellular automaton, is the paradigm of a self-organized critical system. Its underlying abelian structure was discovered by Dhar [2] and Creutz [3]. Other approaches to this model can be found in [4, 5, 6, 7].

We can briefly describe this model as follows : take a regular two-dimensional lattice and on each cell, put some grains. If the number of grains is greater or equal than four, then take four of the grains and put one on each of the neighbor's cell. We say that the - unstable - vertex topples. If a grain falls out of the lattice then it is lost. This corresponds to all boundaries open and could be represented by a special cell which could never be toppled. We call such a cell the *sink*. An addition of one grain can induce a high number of different topplings all over the lattice before reaching a stable configuration - a configuration with no unstable vertex -. This process is finite and is called *relaxation*. The multi-set of topplings involved during the relaxation is called

the *avalanche*. Then we can plot the avalanche - number of topplings involved during the relaxation - distribution under the addition of a grain on a random cell of the lattice. With all the boundaries open, this distribution has a power law tail [8]. Therefore the sandpile model shows the same behavior as many systems seen in the nature [9] (real sand piles, earthquakes or solar flares for example).

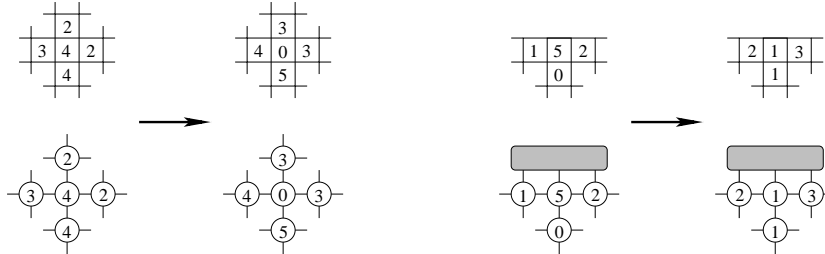


Fig. 1. Graph representation of the sandpile model on the lattice with open boundary conditions. Toppling rule for a regular cell and for a cell near the border. The sink is represented by a gray vertex.

The motivation of our work comes from the observation of a strange phenomenon that occurs when we change the boundary conditions. In some cases, one can observe peaks in the avalanche distribution. Figure 2 shows two avalanche distributions on the 10×3 lattice. For the first case, there are usual - open - boundary conditions. The second case corresponds to special boundary conditions that we call (*) for convenience: there is a closed top boundary, an open bottom boundary and a periodic boundary condition in the horizontal direction.

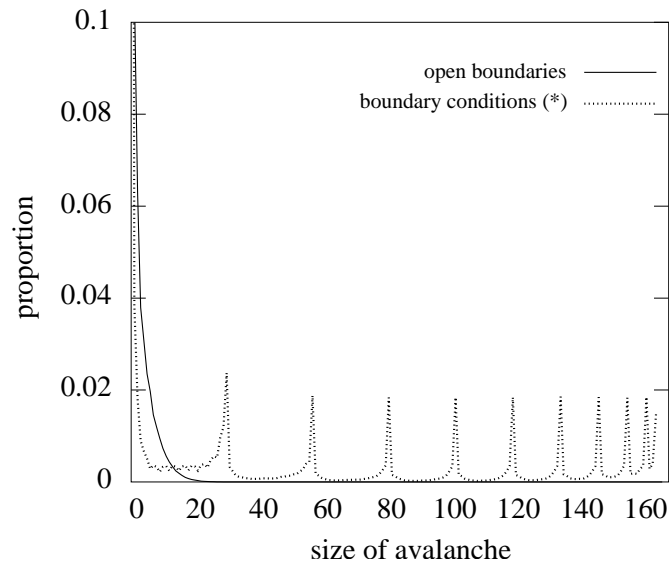


Fig. 2. Avalanche distribution on the 10×3 lattice with the usual - open - boundary conditions on one hand, and with boundary conditions (*) - a closed top boundary, an open bottom boundary and a periodic boundary condition in the horizontal direction - on the other hand.

We will refer to a $n \times k$ lattice with boundary conditions $(*)$ as a (n, k) -wheel, noted $\mathcal{R}(n, k)$. Hence parameter n denote the period along the x -axis, and parameter k the distance between the closed and the open border. Figure 3 gives an example of a $(8, 3)$ -wheel.

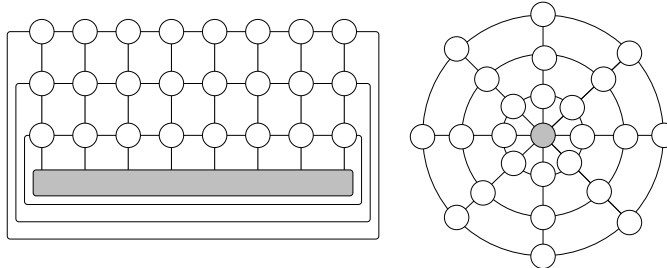


Fig. 3. Two ways of seeing the $(8, 3)$ -wheel.

Experimentally, the avalanche distribution is computed by iterating the following process, starting from the empty configuration:

- (1) add one grain on a random site,
- (2) relax to a stable configuration.

This process is a Markov chain. The stable configurations corresponding to recurrent states of this Markov chain are called recurrent themselves.

The set of recurrent configurations has a group structure (the sandpile group) with a natural addition, and every element of this group can be characterized by Dhar's criterion [10]. We denote $SP(\mathcal{G})$ the sandpile group associated to a graph \mathcal{G} . Moreover, there are as many recurrent configurations as spanning trees. Two bijective proofs exist [11].

The distribution diagrams presented in this paper - like Figure 2 for instance - are obtained after 1 million of iterations. In all our cases, this number is high enough to get good accuracy for the curves.

The paper is divided in two sections. In section 1 we study the case of the simple wheel - $(n, 1)$ -wheel -. For this graph, we show that recurrent configurations could be seen as words of a regular language. Then we explain how to determine the exact avalanche distribution with the help of transducers. In section 2 we study the general (n, k) -wheel for some particular values of the parameters that imply a distribution diagram with peaks. We give an explanation of the last peak observed that could be generalized for other ones.

1 Simple wheel

1.1 Word representation of recurrent configurations

In this section we consider the simple wheel - $(n, 1)$ -wheel -, often referred as the wheel in the literature. It corresponds to the case $k = 1$. By introducing a word representation of the configurations of the wheel, one can study the set of recurrent configurations by studying the corresponding language, *i.e.* set of words. Let choose a random site v . We will refer to it as site 1. The other sites

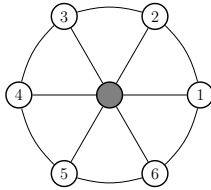


Fig. 4. Simple wheel (case $n = 6$) and a numeration of its vertices.

are defined by an orientation put on the plan (let say the trigonometric one for instance). Such a numeration is shown on Figure 4 for the 6-wheel. Thus we can associate a unique word of $\{0, 1, 2\}^n$ to each stable - resp. recurrent - configuration. Given a stable configuration, we define the word w as $w = w_1 \dots w_n$ such that w_i is the number of grains on site i . We will denote by \mathcal{L} the language corresponding to words associated to recurrent configurations on simple wheels of any size: a word of length n belongs to \mathcal{L} if and only if it corresponds to a recurrent configuration of the n -wheel. Applying Dhar's criterion [10], Cori and Rossin [7] showed that a configuration on the wheel is recurrent if and only if the following two properties hold:

- there is at least one site with two grains,
- between any two sites with no grain, there is at least one site with two grains.

These properties on configurations can easily be expressed in term of corresponding words. Indeed Cori and Rossin computed a valid, simple and non-ambiguous automaton (shown in figure 5) which recognizes the language \mathcal{L} .

Definition 1 A deterministic finite automaton is a 5-uplet (A, S, q, O, δ) , where A is a finite alphabet - set of letters -, S is a finite set of states, q is a special state of S called initial state, O a subset of S of out-states, and δ an application from $S \times A$ to S called transition function.

Usually an automaton is represented by a graph: each element of S is a state of the graph. The initial state is pointed by an in-arrow - without label -, and the out-states are double circled. At last, oriented arrows between states

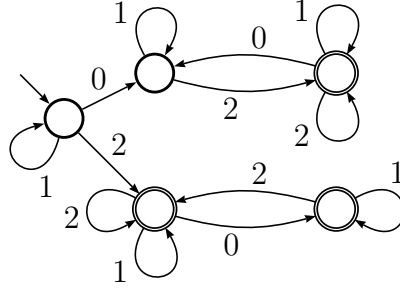


Fig. 5. Automaton recognizing \mathcal{L} .

represent the transition function. They are labeled by a letter, *i.e.* by an element of the alphabet A .

To any automaton with alphabet A , we associate a language on A - a set of words on A - that the automaton is said to recognize. To know if a word w belongs to the language recognized by an automaton, begin at the initial state of the automaton - the one with an in-arrow -. Then, for each letter w_i of w follow the arrow labeled by w_i and if at the end of this process you arrive in an out-state - a double circled one - then the word w belongs to the language. On the other hand if you cannot read a letter - no arrow labeled by w_i - or if the last state is not an out-state then the word is not in the language. For example, the word 12 belongs to \mathcal{L} , but the word 1020 does not: the reading stops in a state that is not an out-state.

Theorem 1 *There exists a deterministic finite automaton that recognizes a language L if and only if L is a regular language.*

Proof : cf [12]. \square

In particular, since \mathcal{L} , the language of words corresponding to recurrent configurations, is recognized by a deterministic finite automaton, it is a regular language. The main reason to work with the word representation and all the theory on regular languages and automata, is that the length of an avalanche on a recurrent configuration has a simple expression in term of the associated word. Suppose that a recurrent configuration has an avalanche of size $m > 0$ when adding a grain on site i , then it is clear that $w_i = 2$ and that there exists a unique $k \geq 0$ such that $w_{i-k} = w_{i-k+1} = \dots = w_i = \dots = w_{i-k+m-1} = 2$ ¹. In other words, site i belongs to a greatest sub-sequence of 2 of length m if $m < n$, and of length $n-1$ or n if $m = n$ - for words of the form 2..212..2, there is one greatest sub-sequence of 2 of length $n-1$, but if one grain is added on a site containing 2 grains, the avalanche will be of size n -. Thus counting these greatest sub-sequences of 2 is equivalent as finding the avalanche distribution on the set of recurrent configurations.

¹ indices must be considered in $\mathbb{Z}/n\mathbb{Z}$

The next section explains how to count automatically greatest sub-sequences of 2 in a language, *i.e.* to determine for each pair of values $m, n \geq 0$ the number of words of length n in the language that contain a greatest sub-sequence of 2 of size m , counted with multiplicity.

1.2 Counting greatest sub-sequences of 2 in a - regular - language

1.2.1 General frame of the method

To count greatest sub-sequences of 2 in a language \mathcal{L} means to find a serie $\mathcal{S} = \sum_{m,n \geq 0} a_{m,n} x^m y^n$ such that $a_{m,n}$ is the number of words of length n in \mathcal{L} that contains a greatest sub-sequence of 2 of length m , counted with multiplicity. As we have seen, to be given a regular language or a finite automaton is the same. Similarly, to be given such a serie is equivalent as to be given a transducer.

A *transducer* is basically an extension of an automaton but the arrows are labeled by both a letter and an expression, and each time you read a letter you output the corresponding expression. But the transducers are not deterministic. So there are multiple paths to read a word. Then the expression produced when reading a word is the sum of the expressions output by the transducer when reading the word on each path. See e.g. Figure 6 for an example.

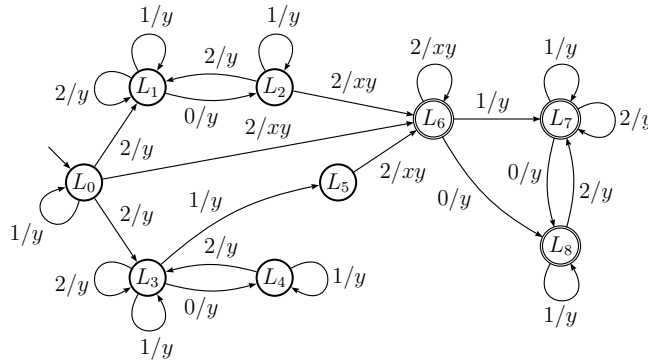


Fig. 6. Transducer T^2 .

In this transducer, read the word 2202. There are two different paths reaching an out-state - L_6 , L_7 or L_8 -. The first one is $L_0L_1L_1L_2L_6$ and the second one $L_0L_6L_6L_8L_7$. The first path gives the monomial xy^4 and the second one x^2y^4 . Notice that the path $L_0L_3L_3L_4L_3$ gives no monomial, because L_3 is not an out-state. The power of x gives the length of a greatest sub-sequence of 2 and the power of y the number of letters of the word.

In this section, we exhibit an algorithm which takes as input an automaton and as output gives a transducer.

1.2.2 Application to the case of \mathcal{L}_2

As an example, we will apply the method to the case of \mathcal{L}_2 , the language recognized by the automaton of Figure 7. \mathcal{L}_2 is a sub-language of \mathcal{L} - for inclusion -. We note $\mathcal{S}_2(x, y)$ the associated serie.

The basic idea is to start with a non-ambiguous automaton which recognizes the language - hence it works only for regular language -. We say that an automaton is non-ambiguous if there is only one way - path - to read a word on it. For any automaton, there exists a non-ambiguous automaton that recognizes the same language.

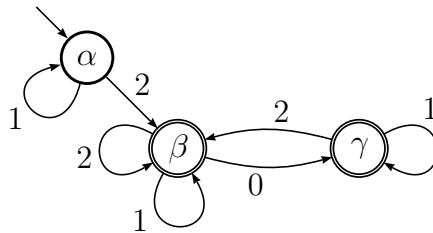


Fig. 7. Non-ambiguous automaton recognizing \mathcal{L}_2 .

The reader familiar with transducer will notice that the transducer of Figure 6 is the one needed to compute $\mathcal{S}_2(x, y)$.

The algorithm to build the transducer from the automaton is the following: each time you have a transition labeled with 2 which can be the starting of a sequence of 2 then duplicate the next states in order to have two different paths. The first one which counts the sequence of 2 beginning at this point and the other one which will count further sequences. Take for example the language $2^+01^*2^+$. A non-ambiguous automaton recognizing this language is given in Figure 8 as well as the associated transducer. Notice that the two loops labeled with 2 could not be the beginning of a sequence of 2.

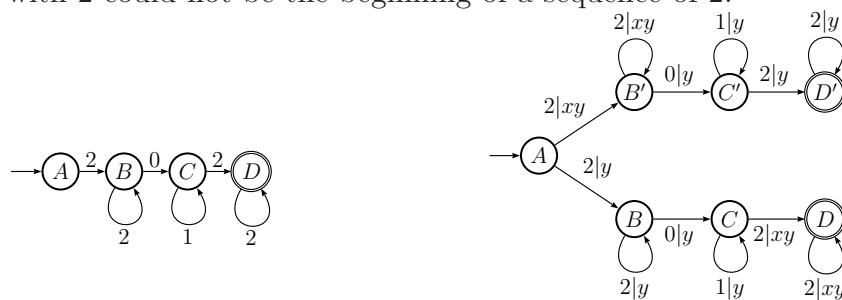


Fig. 8. Simple non-ambiguous automaton for $2^+01^*2^+$ and the associated transducer.

So, take each edge of the automaton recognizing \mathcal{L}_2 and for each one which can be the beginning of a sequence of 2 draw the associated transducer which counts only this sequence. Figures 9,10,11 show the three transducers built

from the three 2-edges $\alpha - \beta$, $\beta - \beta$ and $\gamma - \beta$ of the automaton represented in Figure 7.

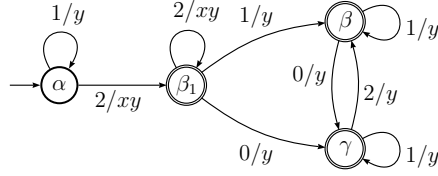


Fig. 9. Transducer associated with edge $\alpha - \beta_1$

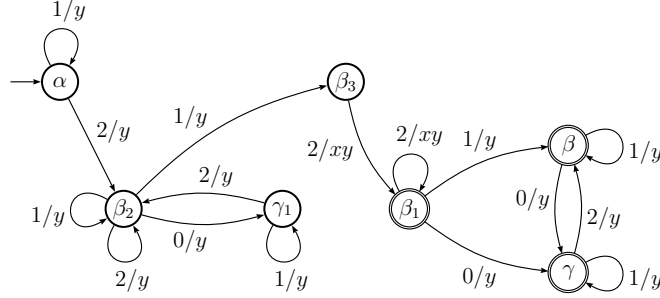


Fig. 10. Transducer associated with $\beta_3 - \beta_1$

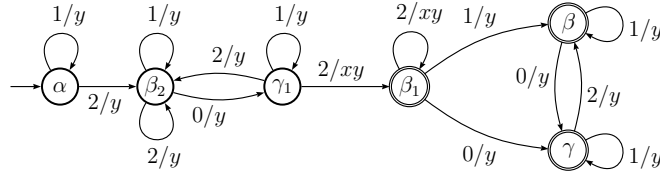


Fig. 11. Transducer associated with edge $\gamma_1 - \beta_1$

For each of these edges, we first duplicate some part of the automaton in order to isolate any greatest sub-sequence of 2 beginning with it, and to discriminate the graph before and after taking the edge. We have then created a 2-edge separator (the three edges pointing to β_1 in figures 9, 10, 11 - $\alpha - \beta_1$, $\beta_3 - \beta_1$ and $\gamma_1 - \beta_1$). Then we can label by $2/xy$ the 2-labeled sub-path beginning by this separator. We also have to make non-final all the states that are before it (states β_2 , β_3 and γ_1 in Figure 11, and states β_2 and γ_1 in Figure 10 are no more out-states). As a consequence, each accepted word has one of its greatest sub-sequence of 2 counted, because a greatest sub-sequence of 2 has to be counted to reach an out-state. For the other edges, we add $/y$ to their label, to count the letters.

Then, we can merge the transducers, and we get the expected result. For example, the transducer \mathcal{T}^2 in Figure 6 is the merged transducer of the three represented on figures 9, 10, 11. We have to pay attention that no greatest sub-sequence of 2 is counted twice, because the starting automaton (Figure 7 in

our example) is non-ambiguous. During the process, this property stays true on pointed-word (word with one of its greatest sub-sequence of 2 pointed). We can say that for such a word, there is only one accepted path, *i.e.* a path leading to an out-state for the word, such that the pointed greatest sub-sequence of 2 is read by the $(2/xy)$ -labeled edges. If the starting automaton is ambiguous, then some greatest sub-sequences of 2 can be counted twice or more.

1.3 Counting the greatest sub-sequences of 2 in a word of \mathcal{L} .

We divide in two the problem and build transducers for \mathcal{L}_2 and $\mathcal{L}_0 = \mathcal{L} \setminus \mathcal{L}_2$ instead of working with a bigger one for \mathcal{L} .

Figure 6 points out a transducer which produces $\mathcal{S}_2(x, y)$. In fact, this serie does not correspond exactly to the expected result: there are some side effects. For example, the word $w = 22011211102212$ gives the contribution $(2x^2 + 2x)y^{14}$ - two greatest sub-sequences of 2 of length 2, and two of length 1 - instead of $(x^3 + x^2 + x)y^{14}$ - one greatest sub-sequence of 2 of length 3, one of length 2 and one of length 1 -. The side effects concern words beginning and

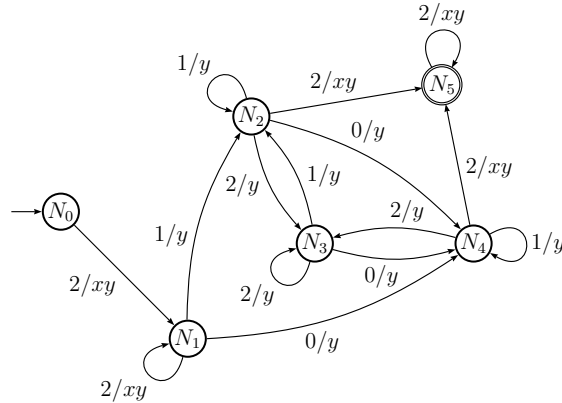


Fig. 12. Transducer \mathcal{T}^+ producing $\mathcal{S}_+(x, y)$.

ending by a greatest sub-sequence of 2 : the transducer of Figure 6 counts the first one and the last one separately instead of merging them. A good way to solve this problem is to consider two other transducers \mathcal{T}^+ and \mathcal{T}^- producing two series $\mathcal{S}_+(x, y)$ and $\mathcal{S}_-(x, y)$, such that $\mathcal{S}_2(x, y) + \mathcal{S}_+(x, y) - \mathcal{S}_-(x, y)$ is the expected result for the special case \mathcal{L}_2 . Figure 12 shows a transducer producing $\mathcal{S}_+(x, y)$.

In what concerns $\mathcal{L}_0 = \mathcal{L} \setminus \mathcal{L}_2$, there are no side effects, and we can apply the method directly. The transducer producing $\mathcal{S}_0(x, y)$ associated to \mathcal{L}_0 is represented on Figure 13.

With all these transducers, we can produce the claimed series - see [12] for details about computing them -. We get the following results:

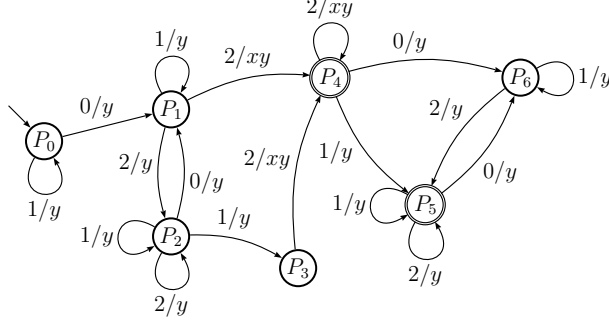


Fig. 13. Transducer \mathcal{T}^0 producing $\mathcal{S}_0(x, y)$.

$$\begin{aligned} \mathcal{S}_2(x, y) &= \frac{xy(1-y)^3}{(1-xy)(1-3y+y^2)^2} \\ \mathcal{S}_+(x, y) &= \frac{x^2y^3(1-y)(2-y)}{(1-xy)^2(1-3y+y^2)} \\ \mathcal{S}_-(x, y) &= \frac{2xy^3(2-y)}{(1-xy)(1-3y+y^2)} \\ \mathcal{S}_0(x, y) &= \frac{xy^2(1-y)^3}{(1-xy)(1-3y+y^2)^2} \end{aligned}$$

It appears that $\mathcal{S}_0(x, y) = y \mathcal{S}_2(x, y)$. Indeed, there is a natural bijection between words in \mathcal{L}_2 of size n and words in \mathcal{L}_0 of size $n + 1$ with the same greatest sub-sequences of 2 - considering the first letter and the last one not being connected -. A word w in \mathcal{L} is either in \mathcal{L}_2 if it begins by a 2 possibly preceded by some 1s or in \mathcal{L}_0 if it begins by a 0 possibly preceded by some 1s. The bijection is the following: let $w = w_1 \dots w_n$ be in \mathcal{L}_2 , then w ends by a 2 or a 0 possibly followed by some 1s. In the first case we define $\Psi(w) = 0w_n \dots w_1$ and on the other case $\Psi(w) = 1w_n \dots w_1$. For both cases, $\Psi(w)$ is in \mathcal{L} . Moreover, it begins by a 0 possibly preceded by some 1s and has length $n + 1$, *i.e.* $\Psi(w)$ is in $\{u \in \mathcal{L}_0, |u| = n + 1\}$. The reciprocal of Ψ is straightforward: if $w' = w'_1 \dots w'_n$ then $\Psi^{-1}(w') = w'_n \dots w'_2$. It results that Ψ is a bijection that also keeps the greatest sub-sequences of 2. That explains why $\mathcal{S}_0(x, y) = y \mathcal{S}_2(x, y)$. A direct corollary is that \mathcal{T}^2 is not minimal. Effectively, we could have built from \mathcal{T}^0 a transducer equivalent to \mathcal{T}^2 with strictly less states.

1.4 Asymptotic analysis of the series and comparison with experimentations

The number of greatest sub-sequences of 2 of size $m > 0$ in words of \mathcal{L} of size n is $[x^m y^n] \mathcal{S}(x, y)$. The exact solution $\mathcal{S}(x, y)$ is:

$$\mathcal{S}(x, y) = \mathcal{S}_2(x, y) + \mathcal{S}_+(x, y) - \mathcal{S}_-(x, y) + \mathcal{S}_0(x, y)$$

One can verify that the following equalities hold:

$$\begin{aligned}
\mathcal{S}(x, y) &= \frac{y^3 - y}{(1 - 3y + y^2)^2} - y - 1 + \left(\frac{1}{1 - xy} \right) \left(\frac{-2y^3 + 3y^2}{(1 - 3y + y^2)^2} + 1 \right) \\
&+ \left(\frac{1}{1 - xy} \right)^2 \left(\frac{y}{1 - 3y + y^2} + y \right) \\
&= \sum_{n \geq m \geq 0} \frac{n}{\sqrt{5}} \left[(\phi^{2(n-m)} - \phi^{-2(n-m)}) x^m - (\phi^{2n} - \phi^{-2n}) \right] y^n \\
&+ \sum_{n \geq 0} x^n y^n + \sum_{n \geq 1} n x^{n-1} y^n \tag{1}
\end{aligned}$$

With expression (1), we can predict the avalanche distribution on the wheel. Indeed, there is a close link between greatest sub-sequences of 2 and avalanche sizes. Let fix n and let take a word w of \mathcal{L} of size n . We define $P_w(x) = \sum_{m=0}^n a_{m,n}^w x^m$ as the polynomial which counts the greatest sub-sequences of 2 of w , and $Q_w(x) = \sum_{m=0}^n l_{m,n}^w x^m$ as the one counting the sizes of the n avalanches that happen, when starting from w , we add a grain on site i and relax, for every site i . Then for any $m > 0$ we have the relations:

$$l_{m,n}^w = m a_{m,n}^w, \text{ if } 0 < m < n - 1, \tag{2}$$

$$l_{n-1,n}^w = 0, \tag{3}$$

$$l_{n,n}^w = (n - 1) a_{n-1,n}^w + n a_{n,n}^w. \tag{4}$$

Indeed, if site i has 2 grains in w , then site i is at the middle of a greatest sub-sequence of 2 of size strictly positive. Let $m > 0$ be the length of this greatest sub-sequence of 2. If $m < n - 1$, for each site of this greatest sub-sequence of 2, the fact to add a grain produces an avalanche of size m . If there are $a_{m,n}$ greatest sub-sequences of 2 of size m , then after the experiment, we have seen $ma_{m,n}^w$ avalanches of size m . Hence $ml_{m,n}^w = l_{m,n}^w$.

If w contains a greatest sub-sequence of 2 of size $n - 1$, there are $n - 1$ avalanches of size n and one of size 0. In this case, $a_{n-1,n}^w = 1$, $a_{n,n}^w = 0$ and $l_{n,n}^w = n - 1$. At last, if $w = 22 \dots 2$, then $a_{n-1,n}^w = 0$, $a_{n,n}^w = 1$ and $l_{n,n}^w = n$.

For $0 < m \leq n$, we define $a_{m,n} = \sum_{w \in \mathcal{L}, |w|=n} a_{m,n}^w$. From equality (1), we get:

$$a_{m,n} = [x^m y^n] \mathcal{S}(x, y) = \begin{cases} \frac{n}{\sqrt{5}} (\phi^{2(n-m)} - \phi^{-2(n-m)}) & \text{if } 0 < m < n - 1 \\ 2n & \text{if } m = n - 1 \\ 1 & \text{if } m = n \end{cases}$$

Let note $\mathcal{A}(x, y)$ the serie corresponding to the avalanche distribution.

The number of recurrent configurations on a simple n -wheel ($|\mathcal{L} \cap \{0, 1, 2\}^n|$) is equal to $(\Phi^n - \Phi^{-n})^2$ [7]. Hence from the definition of $Q_w(x)$, we have the following relation with $\mathcal{A}(x, y)$:

$$\mathcal{A}(x, y) = \sum_{n, m \geq 0} \frac{l_{m, n}}{n(\Phi^n - \Phi^{-n})^2} x^m y^n \quad \text{where} \quad l_{m, n} = \sum_{w \in \mathcal{L}, |w|=n} l_{m, n}^w.$$

For a fixed $m > 0$, relations (2) gives an asymptotic equivalent of the proportion of avalanches of size m when n goes to infinity:

$$[x^m y^n] \mathcal{A}(x, y) \sim \left(\frac{m}{\sqrt{5}} \right) \Phi^{-2m} \quad (5)$$

In particular, it means that the proportion of avalanches of a given size is independent of n asymptotically. Besides, we have:

$$[x^{n-1} y^n] \mathcal{A}(x, y) = 0 \quad \text{and} \quad [x^n y^n] \mathcal{A}(x, y) \sim 2n \Phi^{-2n}$$

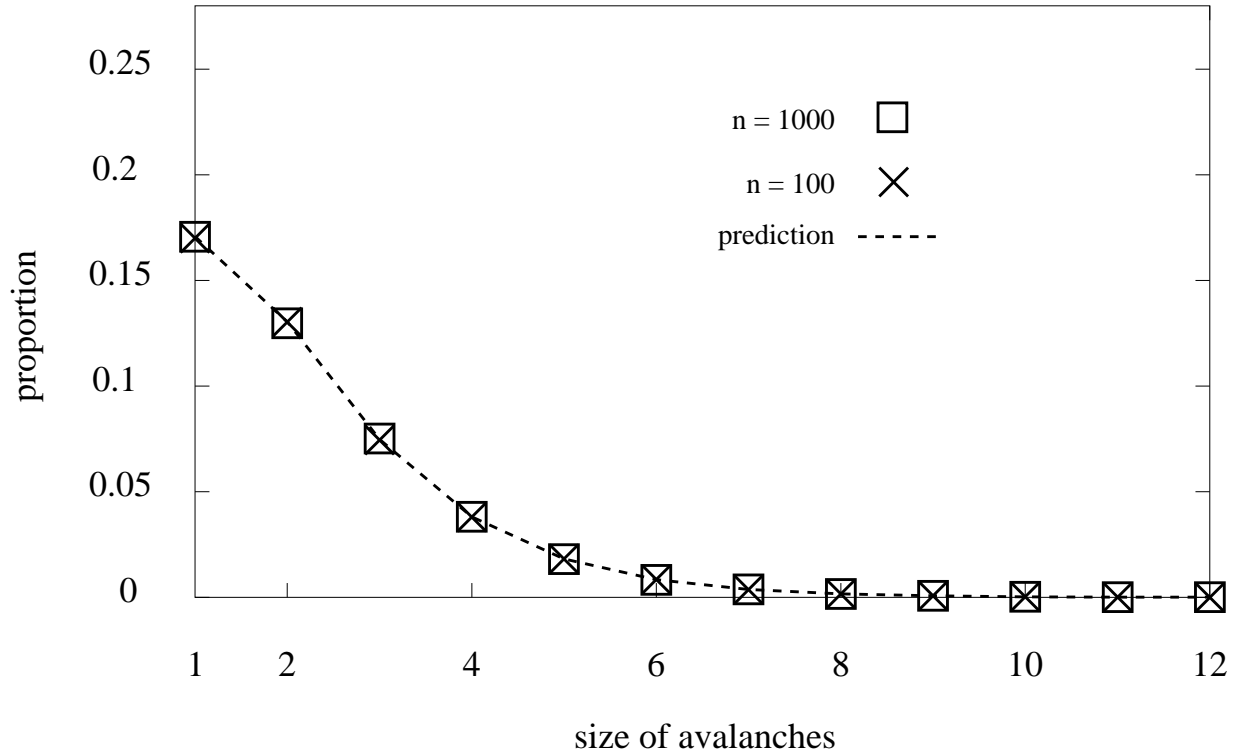


Fig. 14. Avalanche distribution on the n -wheel: expected result (line) and values for $n = 100$ (square) and $n = 1000$ (cross).

To determine the proportion of avalanches of size 0, we use the normalization criterion. As $\mathcal{A}(x, y)$ is the generative serie of a distribution, we have the

relation:

$$\forall n, [y^n] \mathcal{R}(1, y) = 1$$

With equation (5) it gives $[x^0 y^n] \mathcal{A}(x, y) \sim 1 - 1/\sqrt{5}$ for n great enough. In conclusion, at m fixed and when n goes to infinity we have:

$$[x^m y^n] \mathcal{A}(x, y) \sim \begin{cases} \left(\frac{m}{\sqrt{5}}\right) \Phi^{-2m} & \text{if } m > 0 \\ 1 - \frac{1}{\sqrt{5}} & \text{if } m = 0 \end{cases}$$

Figure 14 shows the expected distribution on a line, and the experimental results for $n = 100$ and $n = 1000$ over 10^6 computations. The Independence of the parameter n is clear on the diagram. We present only the values for $m > 0$, because the value for $m = 0$ is much higher. However, in this case also, the predicted value $(1 - 1/\sqrt{5})$ is very well approached with 10^6 computations.

2 Case of the multiple wheel

The study of the avalanche distribution on the general (n, k) -wheel for $k > 1$ is not as easy as in the simple case $k = 1$. Indeed, there is no simple characterization of a recurrent configuration when $k > 1$. Nevertheless the interest is high, because there are peaks in this distribution for some values of the parameters. Figure 15, for instance, shows the avalanche distribution on the $(3, 10)$ -wheel. In this case, we can observe many peaks of similar heights. This phenomenon is very unusual for this type of experiments. The purpose of this section is to show some clues to understand why this phenomenon exists.

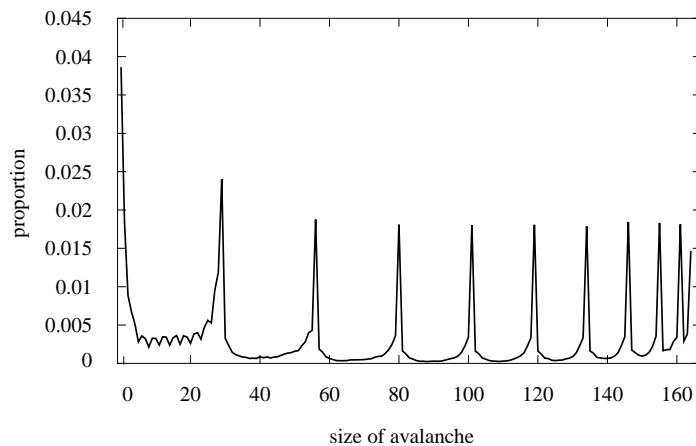


Fig. 15. Appearance of peaks in the avalanche distribution on the $(3, 10)$ -wheel.

This was first observed in [13]. The author shows that there are k unexpected peaks, and that their abscisses are: $x_1 = kn, x_2 = kn + (k - 1)n, \dots, x_k = nk(k+1)/2$. In particular, x_k is the maximal value of the size of an avalanche on the (n, k) -wheel. First we are going to study the last peak, which corresponds to avalanches of size $x_k = nk(k+1)/2$. At last, we explain how the result can be weakly extended to the other peaks.

2.1 Analysis of the last peak

The last peak corresponds to avalanches of maximal sizes. We denote $L(u, i)$ the size of the avalanche obtained after adding a grain at site i to the configuration u and relaxing. We also speak about the size of the avalanche of the element (u, i) . Considering the natural partial order on the set of configurations ($u \leq v \Leftrightarrow u(i) \leq v(i)$ for each site i), a classical result states:

$$u \leq v \implies L(u, i) \leq L(v, i) \text{ for any site } i \quad (6)$$

In fact, this result comes from a stronger property: if a site j has been toppled t times during the avalanche of (u, i) then the same site j has been toppled at least t times during the avalanche of (v, i) . A direct corollary of Property

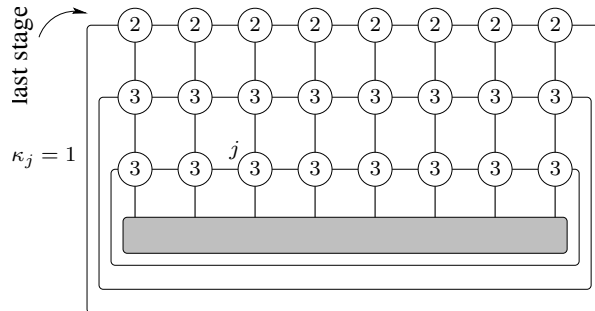


Fig. 16. Configuration r_{max} of the $(8, 3)$ -wheel.

(6) is that x_k is the maximal size of an avalanche. Indeed, there is a unique maximal recurrent configuration r_{max} for the natural partial order on the set of recurrent configurations (every site i is saturated, see Figure 16). For r_{max} we can compute the size of any avalanche in function of the site at which we add the grain. We have: $L(r_{max}, i) = n\kappa_i(2k + 1 - \kappa_i)/2$, where κ_i is the distance from site i to the open boundary. Hence the size of the avalanche is maximal if and only if we add the grain at a site near the closed boundary. We can apply Property (6) to any recurrent configuration u ($u \leq r_{max}$). If the element (u, i) has an avalanche of size x_k , then i is necessarily a site near the closed boundary. Figure 17 expresses this last property: we run the same experimentation, but the random site is always chosen among those that are near the closed boundary. As expected, the last peak seems to appear entirely.

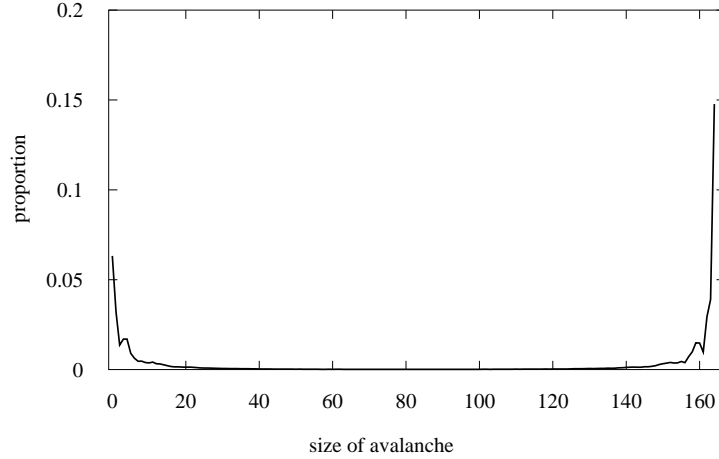


Fig. 17. Random site i is always taken among sites of the last stage. The last peak for the $(3, 10)$ -wheel appears entirely (rate coefficient of $1/k$, here $1/10$).

At this point, if $L(u, i) = x_k$, we can say that i is near the closed border. What can we say about the configuration u ?

Still from the property mentioned above, we know that a site j topples κ_j (distance from j to the open boundary) times during the avalanche of the element (u, i) . After the avalanche, the sites near the closed border are the only one being modified: they all lost 1 grain (except i which was given the extra grain). In term of wheel (cf Figure 3), these sites correspond to the last stage of the wheel. Restricted to this last stage, the configuration u has to be very similar to r_{max} . Indeed, it may contain at most one site different from i with only 1 grain called i' , and the others containing 2 grains, since after the $nk(k+1)/2$ topplings, the configuration obtained has to be recurrent (and at this point only site i among sites of the last stage contains 2 grains).

With the same argument, we get informations on the induced configuration u' of $\mathcal{R}(n, k-1)$, corresponding to the sites at distance at least 2 from the closed boundary. If i' exists, then the configuration u' belongs to $SP(\mathcal{R}(n, k-1))$. On the contrary, if no site of the last stage contains strictly less than 2 grains, then the configuration u' of $\mathcal{R}(n, k-1)$ is either recurrent or equals to a recurrent configuration with one grain less on a site j of the last stage of $\mathcal{R}(n, k-1)$ and which is not a neighbor of site i . Putting this two remarks together, we can find a major value $M(n, k)$ and a minor value $m(n, k)$ of the proportion \mathcal{P} of elements (u, i) whose avalanche size equals x_k . We have:

$$\mathcal{P} \geq \frac{n(n-1)|SP(\mathcal{R}(n, k-1))| + n|SP(\mathcal{R}(n, k-1))|}{nk|SP(\mathcal{R}(n, k))|}$$

$$\mathcal{P} \leq \frac{n(n-1)|SP(\mathcal{R}(n, k-1))| + n(1+n-1)|SP(\mathcal{R}(n, k-1))|}{nk|SP(\mathcal{R}(n, k))|}$$

Thus we can take for $m(n, k)$ and $M(n, k)$ the following values:

$$m(n, k) = \frac{n |SP(\mathcal{R}(n, k-1))|}{k |SP(\mathcal{R}(n, k))|}$$

$$M(n, k) = \frac{2n |SP(\mathcal{R}(n, k-1))|}{k |SP(\mathcal{R}(n, k))|}$$

The number of recurrent configurations of the (n, k) -wheel equals the number of spanning trees of a $n \times k$ lattice with boundary conditions (*). Rubey computed this number in a note [14] inspired by a method due to Noam Elkies described and applied to a similar problem by Kenyon and al. in [15]. It gives:

$$|SP(\mathcal{R}(n, k))| = \prod_{r=0}^{n-1} \prod_{s=0}^{k-1} \left(4 - 2 \cos\left(\frac{2r}{n}\pi\right) - 2 \cos\left(\frac{2s+1}{2k+1}\pi\right) \right)$$

This product behaves like an exponential for both n and k . Experimentally, we observe $|SP(\mathcal{R}(n, k))| \sim \exp[\alpha(k + \gamma)(n + \gamma)]$ with $\alpha \sim 1.1674$ and $\gamma \sim -0.8210$. Using this approximation, we get:

$$m(n, k) = \frac{n}{k} e^{-\alpha(n+\gamma)} \quad (7)$$

$$M(n, k) = \frac{2n}{k} e^{-\alpha(n+\gamma)} \quad (8)$$

In particular, if k increases then x_k grows like k^2 , but the proportion of avalanches of size x_k decreases only like $1/k$. In what concerns the parameter n , the behavior is much more common: the decreasing is exponential. We can thus infer that peaks are better to be observed with small values of n and possibly greater values of k . In practice, for $n \geq 4$, the last peak can not be higher than 2%. The value of $m(n, k)$ makes us understand why the distribution could have a great value for x_k . In what concerns the other peaks, we can find similarly a minor value, but with a coefficient $e^{\gamma(n+\gamma)}$. However, it still explains qualitatively why peaks appear. On the other hand, we can not really explain why they vanish, because we can not as easily obtain a major value. It comes from the fact that avalanches of size x_i for $i < k$ can be the result of the addition of a grain on the j -th stage, with $j > i$. This phenomenon can not exist when $i = k$. It seems even seldom for $i < k$ as Figure 17 makes us think, but we can not exclude it.

Conclusion

In this paper, we have completely characterized the sandpile model on the simple wheel, a $n \times 1$ lattice with unusual boundary conditions. In particular, we can predict the exact avalanche distribution. The set of recurrent

configurations can be coded by a regular language. Thus, we built transducers to produce statistics on words of this language that are closely linked to avalanche size on corresponding recurrent configurations.

Although complete, the $k = 1$ case is of interest not as important as in the general case, in so far as some peaks in the avalanche distribution can be seen for particular values of the two parameters, excluding $k = 1$. But the precedent method can not be applied to the general case $k > 1$. Indeed, there is no precise characterization of recurrent configurations in this case. However, it is possible to interpret the peaks by a qualitative approach. In particular, we found a minor value and a major value of the height of the last peak, which enable us to explain the phenomenon. This could be generalized to the other peaks with less accuracy.

Acknowledgement

We thank our colleague Christian Choffrut for his help on transducers, and Martin Rubey for useful remarks.

References

- [1] P. Bak, C. Tang, and K. Wiesenfeld. Self-organized criticality: an explanation of $1/f$ noise. *Phys. Rev. Lett.*, 59, 1987.
- [2] D. Dhar, P. Ruelle, S. Sen, and D. Verma. Algebraic aspects of abelian sandpile models. *Journal of Physics A*, 28:805–831, 1995.
- [3] M. Creutz. Abelian sandpile. *Computers in Physics*, 5:198–203, 1991.
- [4] N. L. Biggs. Chip-firing and the critical group of a graph. *Journal of Algebraic Combinatorics*, 9(1):25–45, 1999.
- [5] N. L. Biggs. Chip-firing on distance-regular graphs. *Tech. Report LSE-CDAM-96-11, CDAM Research Report Series*, June 1996.
- [6] A. Björner, L. Lovász, and P.W. Sjö. Chip-firing games on graphs. *European Journal of Combinatorics*, 12(4):283–291, 1991.
- [7] R. Cori and D. Rossin. On the sandpile group of dual graphs. *European Journal of Combinatorics*, 21(4):447–459, May 2000.
- [8] D. Dhar. Studying self-organized criticality with exactly solved models. *cond-mat/9909009*, 1999.
- [9] P. Bak. How nature works - the science of soc. *Oxford university press*, 1997.
- [10] D. Dhar. Self-organized critical state of sandpile automaton models. *Physical Review Letters*, 64:1613–1616, 1990.
- [11] R. Cori and Y. Leborgne. Sand-pile model and tutte polynomial. *Adv. in Appl. Math.*, 30:44–52, 2003.
- [12] J. E. Hopcroft and J. D. Ullman. *Introduction to Automata Theory, Languages, and Computation*. Addison-Wesley, Reading, Massachusetts, 1979.
- [13] G. Loheac. Eboulements sur la roue. Technical report, DEA, 2001.
- [14] M. Rubey. Trees of the generalized wheel. *preprint*, 2003.
- [15] R. Kenyon, J. Propp, and D. Wilson. Trees and matchings. *Electronic Journal of Combinatorics*, 7, 2000.